

# Seven years of Raman/backscatter lidar observations of free-tropospheric aerosol layers over Thessaloniki, Greece: Geometrical properties

Elina Giannakaki<sup>1</sup>, Dimitris Balis<sup>1</sup>, Vassilis Amiridis<sup>2</sup>

<sup>1</sup>Laboratory of Atmospheric Physics, Aristotle University of Thessaloniki, 54124, Greece, [egian@auth.gr](mailto:egian@auth.gr)

<sup>2</sup>Institute for Space Applications and Remote Sensing, National Observatory of Athens, I. Metaxa & V. Pavlou, 15236, Penteli, Athens, Greece, [vamoir@space.noa.gr](mailto:vamoir@space.noa.gr)

## ABSTRACT

In this study we present geometrical properties of aerosol particle pollution in the free troposphere over Thessaloniki, Greece. We have used measurements that have been performed using backscatter /Raman lidar from January 2001 to December 2007 in the framework of the European Aerosol Research Lidar Network (EARLINET). In summary we analyze 461 measurements. Specifically, in this work we present statistical information on geometrical properties of free-tropospheric particle layers and its dependence on different air mass sources. In order to do that, we determine the geometrical depth of the particle layers by the use of range corrected backscatter signals at 532 nm. We statistically analyze our measurements by frequency distribution on the basis of all measurements and find out that the most pollution events occur in late spring and throughout the summer months. We have also calculated the frequency distribution of bottom, top, center and depth of the free-tropospheric layers. Finally, we use backward trajectory analysis with Hybrid Single-Particle Lagrangian Integrated Trajectory (HYSPLIT) to identify the main source regions of free tropospheric particles. A pollution event may be characterized with one, two, or more pollution layers from different source regions. For that reason we attribute pollution events to different source regions, if backward trajectories indicate multiple source regions. In the future we shall analyze our 7-year data set for each geometrical layer identified with respect to optical particle properties.

## 1. INTRODUCTION

Aerosols play an important role in the atmospheric radiation budget, in fact, depending on the aerosol type, they can absorb or scatter the incoming and outgoing radiation, warming or cooling the atmosphere and, depending on their size and composition, they can act as condensation nuclei, modifying cloud physical and radiative properties [1]. Despite the importance of free-tropospheric particles on climate and air quality [2] their optical and microphysical properties, their geometrical features, and particle transport mechanisms are still poorly understood.

Aerosol optical depth derived from the Advanced Very High Resolution Radiometer [AVHRR] classified the Mediterranean Sea as one of the areas with the highest aerosol optical depths on the world [3]. Within the eastern Mediterranean, the Aegean sea and the coastal part of continental Greece is in a 'key' geographical position where aerosols from different sources converge, namely maritime aerosols from sea spray; mineral dust from North Africa; and anthropogenic aero-

sols from the highly populated urban centers and industrial areas, as well as biomass burning [4,5] coexist. In the lower troposphere over the Mediterranean, European pollution, that usually originates from local and/or regional emission sources, is mainly responsible for the reduction of air quality, whereas the free tropospheric pollution is often advected over long distances even from other continents [6,7].

## 2. METHODOLOGY

### 2.1 Instrument

The data presented in this study were acquired with a lidar system located at the Laboratory of Atmospheric Physics (LAP) (40.5° N, 22.9° E, 50 m above sea level) in Aristotle University of Thessaloniki (AUTH) from 2001 to 2007. LAP-AUTH lidar system is a 355 nm Raman/elastic lidar system operational since May 2000 in the framework of EARLINET, the first lidar network for tropospheric aerosol study in continental scale [8]. The LAP-AUTH lidar is based on the second and third harmonic frequency of a compact, pulsed Nd:YAG laser, which emits pulses of 300 and 120 mJ at 532 nm and 355 nm, respectively, with a 10 Hz repetition rate [9]. Elastically backscatter signals at both 355 and 532 nm and N<sub>2</sub> Raman shifted signal at 387 nm are collected with a Newtonian telescope of 500mm diameter with 0.7–3 mrad adjustable field-of-view. Three Hamamatsu R7400P-06 photomultipliers are used to detect the lidar signals at 532, 355 and 387 nm with 15m height resolution and 2 min time resolution.

### 2.2 Geometrical Properties of Free-Tropospheric Layers

Range-corrected backscatter signals at 532 nm were used in order to determine the geometrical depth of the particle layers. In those cases where no measurement was available at 532 nm we have used the range corrected signal at 355 nm. In Figure 1, we present an example of how we determine bottom and top height, and thus geometrical depth of the lofted particle layers, for the case of 19<sup>th</sup> of July 2005. We calculate the first derivative of the range corrected signal profile. The top of the planetary boundary layer is defined as the steepest gradient of the profile of the particle backscatter signal, i.e. the largest local minimum of the first derivative of the range-corrected signal (Boesenberg et al., 2003). The top of the planetary boundary layer is determined at about 0.8 km. This height is assumed as the bottom height of the first layer. The derivative shows a first local minimum at about 1.9 km, which is the top of the first layer. There is a second layer with larger particle content directly on top of the

first layer. Thus the bottom height of the second particle layer coincides with the top height of the first particle layer at 1.9 km. The top height of the second layer is indicated by the second local minimum of the derivative profile at about 4.6 km. To test the gradient method we have also used the radiosonde profiles of potential temperature and relative humidity. The temperature and relative humidity profiles as well as the gradient of potential temperature indicate that the bottom and the top of the first layer are about 0.8 km and 1.9 km while the top of the second layer is about 4.4 km.

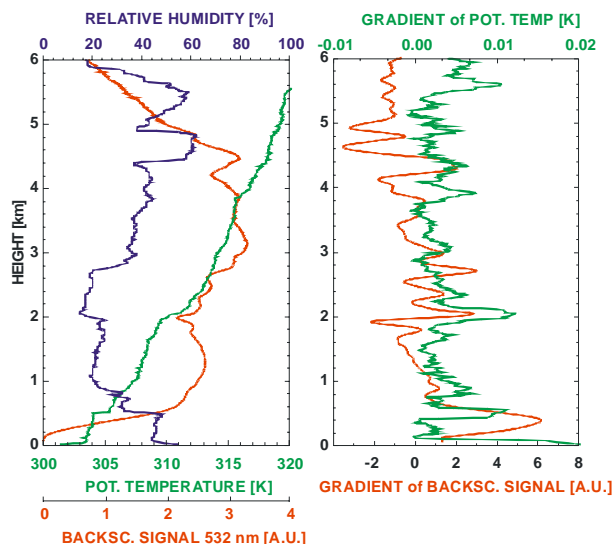


Figure 1. Example of how the heights of the bottom and top are determined with the gradient method. The temporally averaged signal profile (left-red), radiosonde profiles of potential temperature (left-green), relative humidity (left-blue), gradient of the backscatter signal at 532 nm (right-red) and gradient of potential temperature (right-green). The measurement was performed on 19<sup>th</sup> of July 2005 from 10:57 to 12:24 UTC. The radiosonde was launched on 19<sup>th</sup> of July 2005 at 11:51 UTC.

### 2.3 Source Regions of Free-Tropospheric Layers

We use backward trajectory analysis with HYSPLIT (Hybrid Single-Particle Lagrangian Integrated Trajectory) to identify the main source regions of the free tropospheric particles. A discussion of the model is given by Draxler and Hess (1997). HYSPLIT is available at <http://www.arl.noaa.gov/ready/hysplit4.html>.

We calculate four-day backward trajectories calculated for 6 different arrival heights above Thessaloniki, at 0.5, 1.5, 2.5, 3.5, 5.0 and 7.0 km (called from now on trajectory levels). The calculations are made at 12 UTC for the day-time measurements and at 19 UTC for the night-time measurements. In Figure 2 the example of four-day backward trajectory for the 19<sup>th</sup> of July 2005 at 12 UTC is shown. The first layer between 0.8 and 1.9 km corresponds to second trajectory level, this mean at 1.5 km, indicating that air masses are coming from West Europe travelling above continental regions, while the second layer from 1.5 to 4.6 corresponds to 4<sup>th</sup> trajectory level, at 3.5 km, indicating air masses from Saharan region.

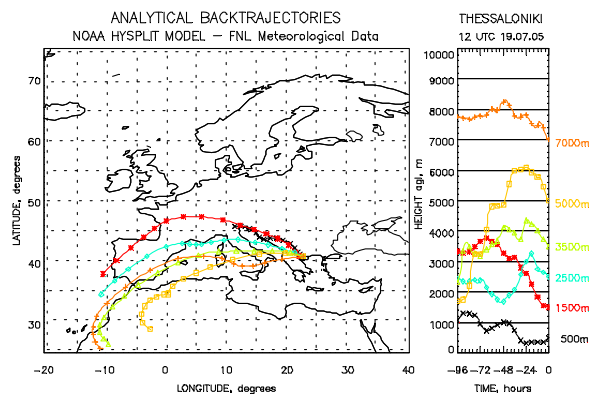


Figure 2. Four-day backward trajectory analysis for 19<sup>th</sup> of July 2005 at 12 UTC.

### 3. RESULTS AND DISCUSSION

Figure 3 shows our complete data set that we acquired from January 2001 until December 2007. The total number of observations is 461. Black vertical lines shows each performed measurement while the red vertical lines indicate the observed free-tropospheric layers from bottom to top. If a plume consisted of several sublayers, the bottom height was calculated for the lowest layer, and the top height was defined by the top of the uppermost lofted layer. The numbers below each year denote the total number of measurements performed in this year, while the percentage corresponds to the number of measurements in which free-tropospheric pollution was observed.

From 461 of the total measurements we observed tropospheric aerosol layers on 313 measurements, corresponding to a percentage of 68%. From the statistics analysis we have found 1 layer at 137 measurements (30%), 2 layers structure at 126 measurements (27%), 3 layers structure at 42 measurements (9%) and finally 4 layers structure at 8 measurements (2%). The number of pollution events in the free troposphere varies considerably among the different years. The minimum number of observations was observed in 2006, while the maximum number of observations was observed during 2002. The geometrical depth of the plumes strongly varies from several hundred meters up to 7 km.

In Figure 4 we present the geometrical features of the lofted particle plumes. The bottom of the lowest free-tropospheric layer is at or below 1.5 km height in 50% of the measurements performed during 2001 – 2007. The top height of the free-tropospheric layers is between 2 and 4 km in 60% of our measurements. The geometrical depth of the aerosol layers is lower or equal to 1.5 km in 73% of the measurements. The center height of the lofted layers follows in a straightforward manner from the frequency distributions of the bottom and top height. We find that in 52% of our measurements the center height of free-tropospheric layers is between 2 and 3.5 km.

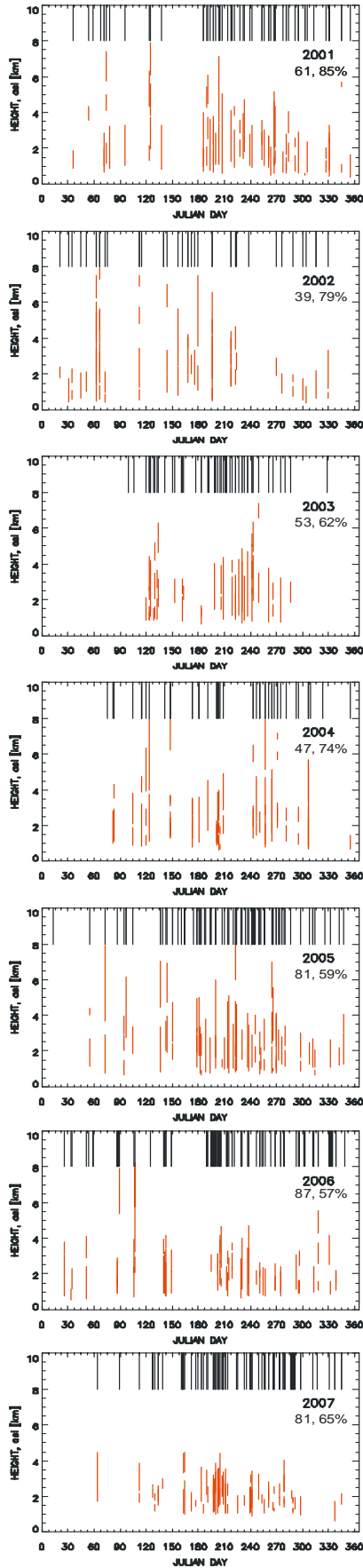


Figure 3. Geometrical depth of lofted particle layers advected to Thessaloniki in years 2001-2007.

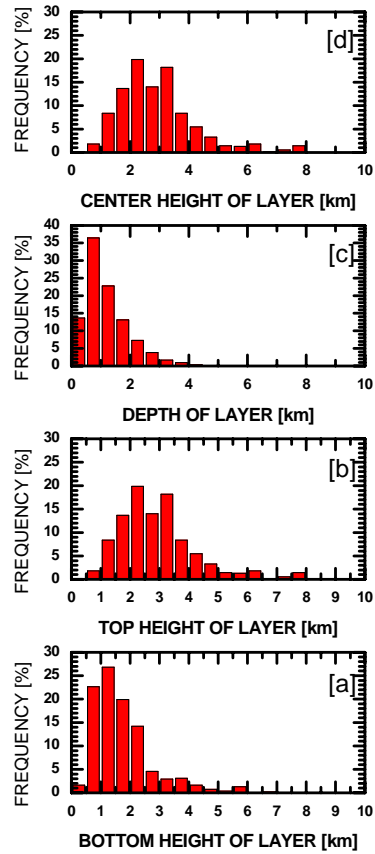


Figure 4. Frequency distribution of [a] bottom height, [b] top height, [c] geometrical depth, and [d] center height of free-tropospheric layers from 2001 to 2007.

In order to classify our measurements to source regions we have computed four-day backward trajectories for each case study.

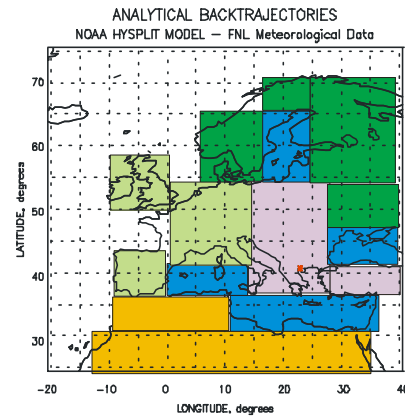


Figure 5. The separation of the observed layers in source areas. Six areas were assumed: Continental NNW (light green), Continental NNE (dark green), Continental Local (Purple), Maritime (blue) and Atlantic Ocean (white).

The computations were made for 6 arrival heights (trajectory levels) and each layer was corresponded to a trajectory level according the center height of the layer as already described in the example of 19<sup>th</sup> of July 2005. We have assumed six different areas Continental NNW, Continental NNE, Continental Local, Maritime,

Sahara desert and Atlantic Ocean as one can see in Figure 5. For each trajectory level we have calculate the number of hours that air mass was traveling across each area region, in order to categorize each observed layer to certain aerosol types taking also into account the direction of air mass.

In Figure 6, we present the total number of hours that air masses were traveling across each source area for each observed layer for the time period from 2001 to 2007. The segregation of measurements into different sources is particularly difficult in our region due to the mixing state of different aerosol types that is usually observed in the free troposphere of Thessaloniki. As one can see from Figure 6, most of the observed layers are being affected by local air pollution of Thessaloniki. Moreover, Thessaloniki is being located in an urban area not far from sea, a large number of observed layers include some 'contamination' by marine aerosols. Although that air masses that originates from Saharan desert are not stay a lot of hours above this region, the 'signature' of desert particles is characterist as many studies have shown.

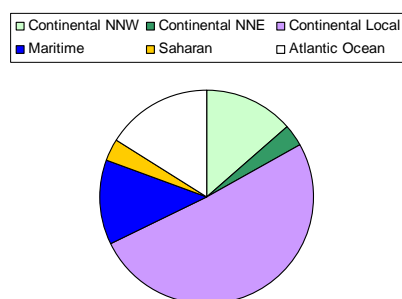


Figure 6. Number of hours that air masses were traveling above each source area for all of the observed layers in the period 2001 - 2007

#### 4. CONCLUSIONS

In this study we summarize the geometrical properties of aerosol particle pollution in the free troposphere over Thessaloniki, Greece during the time period from January 2001 to December 2007. We present the methodology used in the frame of one example in order to determine the bottom and the top of the lofted layers.

We find that in 68% of all 46 measurements lofted pollution layers are present. Most of these events occur during spring and summer of each year. We also find that in 57% of the measurements have one or two layers. The minimum number of observations was observed in 2006, while the maximum number of observations was observed during 2002. The geometrical depth of the plumes strongly varies from several hundred meters up to 7 km. The bottom of the lowest free-tropospheric layer is at or below 1.5 km height in 50% of the measurements performed during 2001 – 2007. The top height of the free-tropospheric layers is between 2 and 4 km in 60% of our measurements. The geometrical depth of the aerosol layers is lower or equal to 1.5 km in 73% of the measurements. The center height of the lofted layers follows in a straightforward manner from the frequency distributions of the bottom and top height. We find that in 52% of our

measurements the center height of free-tropospheric layers is between 2 and 3.5 km.

In the future we shall analyze our 7-year data set for each geometrical layer identified with respect to optical particle properties for each aerosol type.

#### REFERENCES

- [1] Kaufman, Y.J. et al., 2002: A satellite view of aerosols in the climate system, *Nature*, **419**, pp. 215-223
- [2] Jacob, D.J., Logan, J.A. & Murti, P.P. 1999: Effect of rising Asian emissions on surface ozone in the United States, *Geophysical Research Letters*, **26**, no. 14, pp. 2175-2178.
- [3] Husar, R.B., et al. 1997: Characterization of tropospheric aerosols over the oceans with the NOAA advanced very high resolution radiometer optical thickness operational product, *Journal of Geophysical Research*, **102**, pp. 16889-16909.
- [4] Formenti, P. et al., 2002: STAAARTE-MED 1998 summer airborne measurements over the Aegean Sea 2. Aerosol scattering and absorption, and radiative calculations, *Journal of Geophysical Research*, **107**, pp. 2-1-2-14.
- [5] Formenti, P., et al., 2001: Aerosol optical properties and large-scale transport of air masses: Observations at a coastal and a semiarid site in the eastern Mediterranean during summer 1998, *Journal of Geophysical Research*, **106**, pp. 9807-9826.
- [6] Mattis, I., et al. 2004: Multilayer aerosol observations with dual-wavelength Raman lidar in the framework of EARLINET, *Journal of Geophysical Research*, **109**, D13203.
- [7] Müller, D., et al., 2004: Closure study on optical and microphysical properties of a mixed urban and Arctic haze air mass observed with Raman lidar and Sun photometer, *Journal of Geophysical Research*, **109**, D13206.
- [8] Bösenberg, J., et al., 2003: 'EARLINET: 'A European Aerosol Research Lidar Network to Establish an Aerosol Climatology, *Report of the Max-Planck-Institute for Meteorology*, pp. 348.
- [9] Balis, D., et al., 2000: Tropospheric LIDAR aerosol measurements and sun photometric observations at Thessaloniki, Greece, *Atmospheric Environment*, **34**, pp. 925-932.
- [10] Mattis, et al., 2008: Ten years of multiwavelength Raman lidar observations of free-tropospheric aerosol layers over central Europe: Geometrical properties and annual cycle, *Journal of Geophysical Research*, **113**, D 20202.

#### ACKNOWLEDGEMENTS

The financial support for the improvement of the EARLINET infrastructure by the European Commission under grant RICA-025991 is gratefully acknowledged. The authors also acknowledge the ESA financial support under the ESTEC Contract No. 21487/08/NL/HE and the ESRIN Contract No. 21769/08/I-OL.